© 2014. Published by The Company of Biologists Ltd | Development (2014) 141, 2075-2084 doi:10.1242/dev.097790

RESEARCH ARTICLE

Development of the prethalamus is crucial for thalamocortical projection formation and is regulated by Olig2

Katsuhiko Ono[1,*,‡], Adrien Clavairoly[2,*], Tadashi Nomura[1,3], Hitoshi Gotoh[1], Aoi Uno[1], Olivier Armant[4], Hirohide Takebayashi[3,5], Qi Zhang[6], Kenji Shimamura[7], Shigeyoshi Itohara[6], Carlos M. Parras[2] and Kazuhiro Ikenaka[8]

ABSTRACT

Thalamocortical axons (TCAs) pass through the prethalamus in the first step of their neural circuit formation. Although it has been supposed that the prethalamus is an intermediate target for thalamocortical projection formation, much less is known about the molecular mechanisms of this targeting. Here, we demonstrated the functional implications of the prethalamus in the formation of this neural circuit. We show that Olig2 transcription factor, which is expressed in the ventricular zone (VZ) of prosomere 3, regulates prethalamus formation, and loss of Olig2 results in reduced prethalamus size in early development, which is accompanied by expansion of the thalamic eminence (TE). Extension of TCAs is disorganized in the *Olig2-KO* dorsal thalamus, and initial elongation of TCAs is retarded in the *Olig2-KO* forebrain. Microarray analysis demonstrated upregulation of several axon guidance molecules, including *Epha3* and *Epha5*, in the *Olig2-KO* basal forebrain. *In situ* hybridization showed that the prethalamus in the wild type excluded the expression of *Epha3* and *Epha5*, whereas loss of Olig2 resulted in reduction of this Ephas-negative area and the corresponding expansion of the Ephas-positive TE. Dissociated cultures of thalamic progenitor cells demonstrated that substrate-bound EphA3 suppresses neurite extension from dorsal thalamic neurons. These results indicate that Olig2 is involved in correct formation of the prethalamus, which leads to exclusion of the EphA3-expressing region and is crucial for proper TCA formation. Our observation is the first report showing the molecular mechanisms underlying how the prethalamus acts on initial thalamocortical projection formation.

KEY WORDS: Dorsal thalamus, Thalamic eminence, EphA3, Microarray, *In situ* hybridization, Mouse

INTRODUCTION

The cerebral cortex and dorsal thalamus have reciprocal connections, which are essential morphological bases for cortical functions. Thalamocortical axons (TCAs) send sensory information and feedback of motor programming from the caudal brain areas, and these connections are organized in a topographical manner (Vanderhaeghen and Polleux, 2004). Formation of the topographic connections is regulated by several axon guidance molecules (Braisted et al., 2000, 2009; Dufour et al., 2003; Vanderhaeghen and Polleux, 2004; Torii and Levitt, 2005; Uemura et al., 2007). Developing thalamic neurons send axons towards the ventral telencephalon through the prethalamus (or ventral thalamus). Special guidance cells named corridor cells in the ventral telencephalon guide TCAs to the pallium (López-Bendito et al., 2006). Thus, the ventral telencephalon is regarded as an important intermediate target for the formation of reciprocal connections.

TCAs need to pass through the prethalamus on exiting from the dorsal thalamus to the ventral telencephalon as the prethalamus occupies exiting points of TCAs. The prethalamus has been supposed to be an intermediate target of TCAs (Deng and Elberger, 2003; Molnár et al., 2012); however, evidence is scarce that identifies the molecular mechanisms underlying the axon guidance role of the prethalamus, and functions of the prethalamus in thalamocortical projection are not fully understood (Leyva-Diaz and Lopez-Bendito, 2013). Mouse lines showing defects in prethalamus formation would be a useful model for analyzing the functional role of the prethalamus in thalamocortical projection formation.

Olig2 is a bHLH transcription factor that is essential for oligodendrocyte and somatic motoneuron development (Lu et al., 2002; Takebayashi et al., 2002b; Zhou and Anderson, 2002), and is also involved in dorsoventral patterning of the spinal cord, which is required for pMN domain specification. In the diencephalon, Olig2 is expressed in the VZ of the prethalamus at early fetal stages, such as E9.5 in mice (Ono et al., 2008). These Olig2+ cells differentiate into GABAergic neurons in the thalamic reticular nucleus (TRN) as well as into macroglial cells in the diencephalon, whereas loss of Olig2 does not affect GABAergic neuron differentiation (Takebayashi et al., 2008). The function of Olig2 in this area has not been elucidated. Here, we report that loss of Olig2 results in hypoplasia of the prethalamus, which leads to defects of TCA extension. The prethalamus is devoid of *Epha3* and *Epha5* expression whereas ventrally adjacent thalamic eminence (TE) expresses *Epha3* and *Epha5* (referred to here as Ephas positive) and, in the E13.5 *Olig2-KO* diencephalon, Ephas-positive TE expanded dorsally. Furthermore, the substrate-bound Epha3 suppresses neurite extension in cultured thalamic neurons. These results together indicate that Olig2 regulates proper formation of the prethalamus, which leads to exclusion of the EphA3-expressing non-permissive region for TCA and is crucial for proper TCA formation.

RESULTS

Reduced size of the prethalamus in *Olig2-KO* mice

We first explored early development of the prethalamus in the *Olig2-KO* mouse to examine whether *Olig2-KO* mice can be used to

[1]Department of Biology, Kyoto Prefectural University of Medicine, Kyoto 603-8334, Japan. [2]Sorbonne Universités, UPMC Univ Paris 06 UMR S 1127, and Inserm U 1127, and CNRS UMR 7225, and ICM, 75013, Paris, France. [3]PRESTO, JST, Kawaguchi 332-0012, Japan. [4]Institute of Toxicology and Genetics, KIT Campus Nord, Eggenstein-Leopoldshafen D-76344, Germany. [5]Division of Neurobiology and Anatomy, Graduate School of Medical and Dental Sciences, Niigata University, Niigata 951-8510, Japan. [6]Laboratory for Behavioral Genetics, RIKEN BSI, Wako 351-0198, Japan. [7]Department of Brain Morphogenesis, Institutes for Molecular and Embryological Genetics, Kumamoto University, Kumamoto 860-8556, Japan. [8]Division of Neurobiology and Bioinformatics, National Institute for Physiological Sciences, Okazaki 444-8787, Japan.
*These authors contributed equally to this work

[‡]Author for correspondence (katsono@koto.kpu-m.ac.jp)

Received 19 April 2013; Accepted 11 March 2014

Development (2014) 141, 2075-2084 doi:10.1242/dev.097790

analyze functions in the prethalamus for thalamocortical projection formation. The prethalamus is demarcated by *Dlx2*, as well as by Islet1/2, expression (Bulfone et al., 1993).

As Olig2 expression in the diencephalon is observed as early as E9.5 (Ono et al., 2008; supplementary material Fig. S1), whole-mount *Dlx2 in situ* hybridization was performed in the E10.5 forebrain. *Dlx2*+ prethalamus was much smaller in *Olig2-KO* mice (n=3) than in wild-type animals (n=4) (Fig. 1A,B, arrows). To observe prethalamus formation more precisely, coronal sections of the E11.5 forebrain were double-stained with *Dlx2 in situ* hybridization and Islet1/2 immunohistochemistry. In wild-type or heterozygous mice, *Dlx2*+ cells were observed in the middle part of the diencephalon (Fig. 1C,E,G,I). Islet1/2+ cells were located laterally to *Dlx2*+ cells (Fig. 1I). Because no significant difference was observed between wild-type and Olig2 heterozygous animals, they are both referred to as normal control animals. *Dlx2*+ cells in the *Olig2-KO* diencephalon were also observed at a similar level; however, as shown in the whole-mount *in situ* hybridization, the *Dlx2*+ area was much smaller than that in normal control animals (Fig. 1D,F,H,J). The mean area of the *Dlx2*+ region in each section of *Olig2-KO* was ~60% smaller than that of the wild type (Fig. 1K). In addition, the Islet1/2+ region was also greatly decreased in the *Olig2-KO* prethalamus (Fig. 1I,J). The prethalamus in E13.5 *Olig2-KO* mice was also smaller (not shown); thus, loss of Olig2 results in hypoplasia of the prethalamus in early development, as early as E10.5.

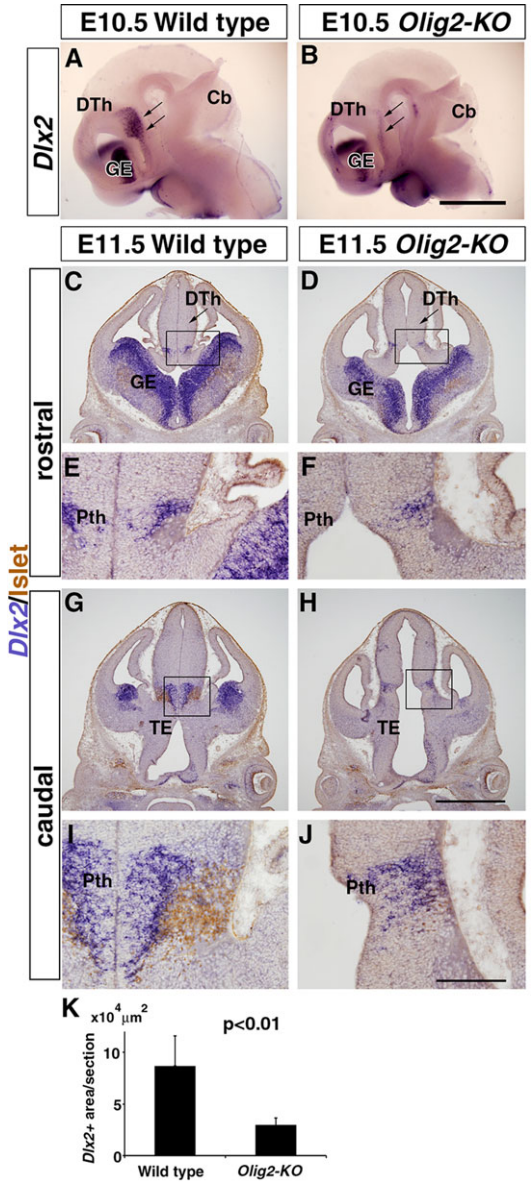

Fig. 1. Defective prethalamus development in the *Olig2-KO* mouse. (A,B) Whole-mount *in situ* hybridization of E10.5 forebrain with *Dlx2*. Arrows indicate prethalamus. The prethalamus of the *Olig2-KO* mouse shows hypoplasia. (C-J) Double staining with *Dlx2 in situ* hybridization (purple) and Islet1/2 immunohistochemistry (brown). (C,E,G,I) E11.5 wild-type mouse. (D,F,H,J) E11.5 *Olig2-KO* mouse. The *Dlx2*+ and Islet1/2+ area is much smaller in *Olig2-KO* mouse than in normal control animals. Cb, cerebellum; DTh, dorsal thalamus; GE, ganglionic eminence; Pth, prethalamus; TE, thalamic eminence. (K) Quantitative analysis of E11.5 *Dlx2*+ prethalamus region, showing 60% reduction of the area in the *Olig2-KO* mouse. Data are mean±s.e.m. (wild type, n=3; *Olig2-KO*, n=3; Student's t-test). Scale bars: 1 mm in B; 500 µm in H; 100 µm in J.

We then examined whether reduced proliferation or elevated apoptosis contributes to the hypoplasia of the *Olig2-KO* prethalamus. Sections of control and *Olig2-KO* mice at E10.5 and E11.5 were double labeled with *Dlx2 in situ* hybridization and cleaved caspase 3 immunohistochemistry (a marker of apoptotic cells) or pH3 immunohistochemistry (a marker of mitotic cells). At E10.5, cleaved caspase 3+ spots were more abundantly observed in the prethalamus of *Olig2-KO* than in control mice (supplementary material Fig. S2A-E), whereas pH3+ cell density was similar between the control and *Olig2-KO* (supplementary material Fig. S2G). At E11.5, the density of cleaved caspase 3+ cells was similar between the control and *Olig2-KO* prethalamus, whereas that of pH3+ cells was slightly higher in the *Olig2-KO* prethalamus than in the normal control (supplementary material Fig. S2F,H). These results indicate that transiently elevated apoptosis at E10.5 may be, at least in part, involved in reduction of the size of the prethalamus in *Olig2-KO* mice.

Dorsal shift of the border between the prethalamus and thalamic eminence in the *Olig2-KO* diencephalon

To better understand the defects of prethalamus formation in *Olig2-KO* mice, areas adjacent to the prethalamus were examined by the expression of region marker molecules. The thalamic eminence (TE) is a dorsal part of prosomere 3, although, in coronal sections of the fetal diencephalon, TE is observed ventral to the prethalamus (Fig. 2; López-Bendito and Molnár, 2003; Puelles, 2001). The TE is demarcated by the expression of calretinin (Abbott and Jacobowitz, 1999), Tbr1 and Tbr2 (Eomes – Mouse Genome Informatics) (Bulfone et al., 1995; Puelles, 2001). Tbr2 is expressed in basal progenitors of the TE, and calretinin and Tbr1 are expressed in the mantle layer. In normal control animals, Tbr2 expression was observed ventrally to the Olig2+ domain (Fig. 2A). In the *Olig2-KO* diencephalon, Tbr2 was also expressed ventral to the CreER expression that recapitulates intrinsic Olig2 expression (Fig. 2B), and the Tbr2+ area was much wider than that in normal control animals (Fig. 2A,B, flanked by arrows), whereas the CreER+ prethalamus was narrower (Fig. 2B, flanked by arrowheads). Although *Lhx5* expression was reported to demarcate the prethalamus, in our observation, *Lhx5* was expressed in the dorsal border of the prethalamus and the main body of the TE whereas the main part of the prethalamus was devoid of *Lhx5* expression (supplementary material Fig. S3A,F). In the E12.5 *Olig2-KO* diencephalon, the *Lhx5*-negative area was much reduced in size and was compatible with the reduction of the *Dlx2*+ area (supplementary material Fig. S3B,G). We then measured the relative positions of Tbr2- and Olig2- or Cre-expressing domains within the dorsoventral axis of the E13.5

Development (2014) 141, 2075-2084 doi:10.1242/dev.097790

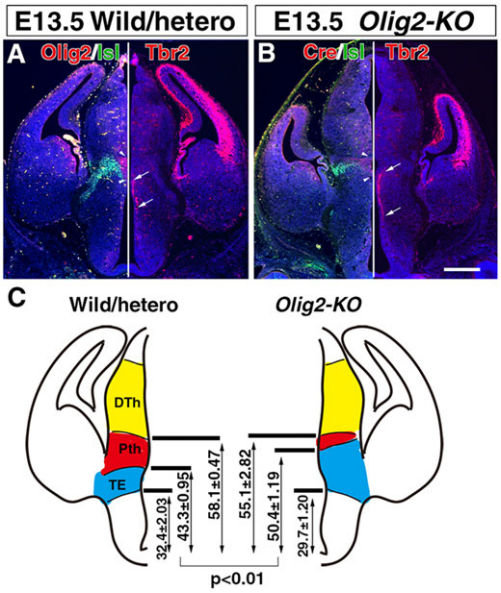

Fig. 2. Altered formation of the prethalamus and TE in *Olig2-KO* mice. (A,B) Comparison of formation of the prethalamus and thalamic eminence in normal control and *Olig2-KO* mouse at E13.5. Both are composite pictures, in which left and right halves are adjacent sections immunostained with Islet1/2 (green in left half), Olig2 or Cre (red in left half), and Tbr2 (red in right half). The prethalamus is shown by Islet1/2 and the TE by Tbr2. The VZ of the prethalamus is indicated by arrowheads and that of the TE by arrows. The mutant embryo brain was taken at a slightly caudal level compared with the wild-type embryo brain. Scale bar: 500 µm in B. (C) Relative position of borders of the dorsal thalamus (yellow), prethalamus (red) and TE (blue) in coronal sections of the diencephalon. Total height of the diencephalon in the coronal section is regarded as 100% height, and relative position is expressed as percentage from the bottom (mean±s.d.; wild type, *n*=3; *Olig2-KO*, *n*=3; Student's *t*-test).

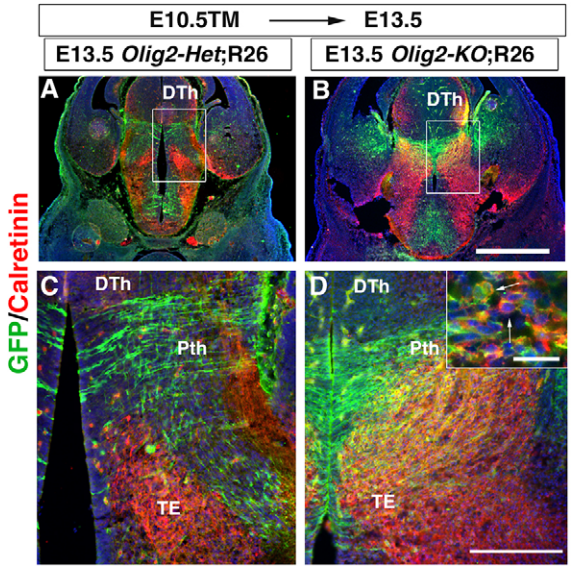

Fig. 3. Fate change of Olig2 lineage cells in the absence of Olig2. (A,B) E13.5 *Olig2-hetero*;Rosa26^{GFP} and *Olig2-KO*;Rosa26^{GFP} mouse diencephalon, stained with calretinin (red) and GFP (green). Boxed areas in A and B are magnified in C and D, respectively. (C,D) Higher magnification pictures. In the heterozygous mouse, GFP+ and calretinin+ cells are mutually exclusive (C), whereas overlapping distribution is apparent in *Olig2-KO* mouse (D). Inset shows representative double-labeled cells (arrows). Scale bars: 500 µm in B; 200 µm in D; 20 µm in inset.

diencephalon (Fig. 2C). Total height of the diencephalon in a coronal section was regarded as 100% height. As shown in Fig. 2C, the dorsal border of the prethalamus and the ventral border of the TE were unchanged in the *Olig2-KO* diencephalon. However, the border between the prethalamus and TE was significantly shifted dorsally in knockout mice. In addition, the Tbr2-expressing thalamic eminence occupied 10±1.44% width within the total height of the diencephalon in control animals, whereas that in *Olig2-KO* mice was 20.7±2.38%, which was also statistically significant (P<0.01). These observations clearly demonstrate hypoplasia of the prethalamus accompanied by expansion of the TE in *Olig2-KO* mice.

To examine whether the reduction of the prethalamus with dorsal expansion of the TE involves a fate change of Olig2 lineage cells, we performed genetic fate mapping. We generated Olig2$^{KICreER/+}$; Rosa26-GAP-EGFP and Olig2$^{KICreER/KICreER}$;Rosa26-GAP-EGFP (hereafter named *Olig2-hetero*;Rosa26^{GFP} and *Olig2-KO*;Rosa26^{GFP}, respectively) mice, and tamoxifen was administered to dams at E10.5 to induce GFP expression in Olig2+ cells. Animals were analyzed at E13.5, and sections were double-stained with calretinin, Tbr1 or Islet1/2 and with GFP immunohistochemistry. In the *Olig2-hetero*;Rosa26^{GFP} diencephalon, GFP+ cells and calretinin+ cells were mostly mutually exclusive and thus only a few cells were double immunoreactive (Fig. 3A,C). By contrast, calretinin+ cells, as well as Tbr1+ cells, expanded dorsally and showed overlapping distribution with GFP+ cells in the *Olig2-KO*;Rosa26^{GFP} diencephalon (Fig. 3B,D; supplementary material Fig. S4A,B), and many calretinin+ cells were also GFP+, indicating a fate change of Olig2 lineage cells (Fig. 3D, inset). Islet1/2+ cells in the *Olig2-KO* prethalamus were also GFP+ (supplementary material Fig. S4C,D) and therefore Olig2 lineage cells in the *Olig2-KO* diencephalon showed dual phenotypes, both prethalamus and TE.

Although the border between the prethalamus and the TE was dorsally shifted in *Olig2-KO* mice, other areas of the forebrain seemed to be properly formed. For example, the *Olig3*+ dorsal thalamus was positioned dorsal to the prethalamus (Vue et al., 2009; supplementary material Fig. S3C,H). Whereas the ventral and dorsal borders of the *Olig3*+ area were unchanged in the *Olig2-KO* mouse (supplementary material Fig. S3C,H), the relative width of the Olig3 domain within the dorsoventral axis was slightly reduced in the *Olig2-KO* diencephalon (supplementary material Fig. S3K). *Shh* and *Fgf8* expression in ZLI was unchanged in the absence of Olig2 (supplementary material Fig. S3D,E,I,J). In addition, Islet1/2+ cells, including corridor cells (López-Bendito et al., 2006), were positioned normally in the ventral telencephalon at E13.5 in both the normal control and *Olig2-KO* mice (supplementary material Fig. S5). Overall, the prethalamus and TE are specifically malformed in the early forebrain development of the *Olig2-KO* mouse, although a slight defect was noticed in the dorsal thalamus.

Defect of TCA extension in the *Olig2-KO* diencephalon

We next examined whether the prethalamus has an impact on the formation of the thalamocortical projection. Axons in the fetal forebrain were stained with anti-neurofilament M (NF-M) antibody. At E13.5, when TCAs start to extend into the prethalamus and the ventral telencephalon (López-Bendito et al., 2006), NF-M+ axons extended dorsoventrally and in parallel in the mantle layer, and they gradually converged in the ventral part (Fig. 4A,B, arrowheads). In age-matched *Olig2-KO* mice, NF-M+ axons were disorganized and followed a tortuous course in the dorsal thalamus; they sometimes formed small aggregates (Fig. 4C,D, arrowheads). To elucidate whether these NF-M+ axons are TCAs, they were co-immunostained with anti-netrin G1 antibody (Niimi et al., 2007) because netrin G1 is

Development (2014) 141, 2075-2084 doi:10.1242/dev.097790

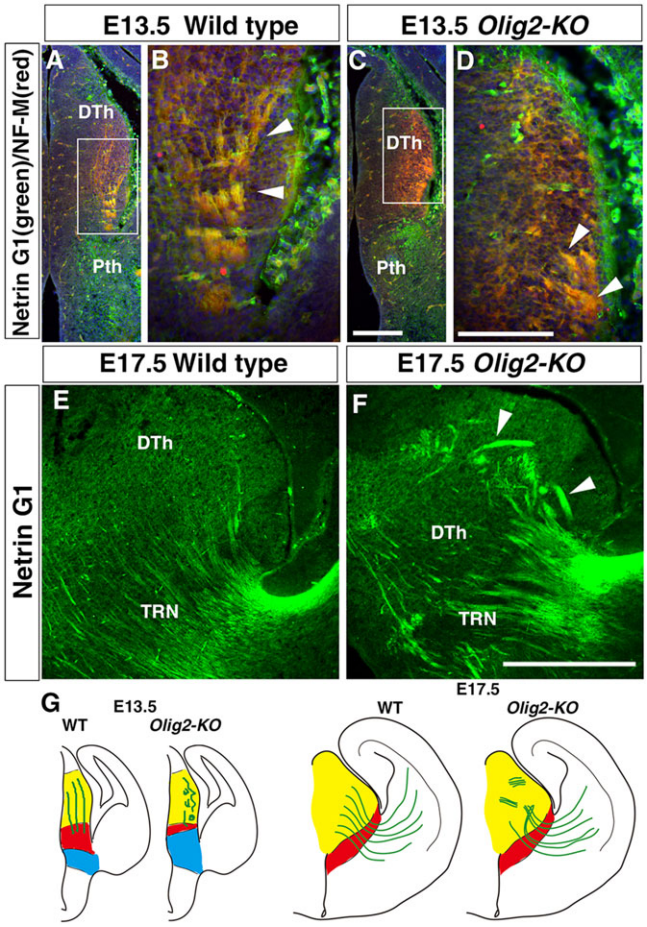

Fig. 4. Disorganization of TCAs in the *Olig2-KO* dorsal thalamus. (A-D) E13.5 diencephalon immunostained with anti-NF-M (red) and anti-netrin G1 (green) antibodies. NF-M+ axons in the dorsal thalamus (DTh) are also netrin-G1+, indicating that they are TCAs. Wild-type TCAs extend in parallel and converge ventrally in the prethalamus (A,B; arrowheads in B). TCAs in the *Olig2-KO* mouse show disorganized extension and sometimes form axon aggregates (C,D; arrowheads in D). (E,F) Netrin G1+ TCAs in the E17.5 DTh and prethalamus (thalamic reticular nucleus, TRN). In the wild type, netrin G1+ axons are extended in parallel in the DTh and TRN (E), whereas those in the *Olig2-KO* mouse form abnormal thick axon bundles orienting randomly (arrowheads in F). (G) Summary of the observed defects in *Olig2-KO* diencephalon. Scale bars: 200 μm in C; 100 μm in D; 500 μm in F.

expressed by developing dorsal thalamic neurons (Nakashiba et al., 2002). Indeed, NF-M+ axons co-expressed netrin G1 in both the wild-type and *Olig2-KO* dorsal thalamus (Fig. 4B,D, arrowheads), indicating that the disorganized axons in *Olig2-KO* mice were TCAs (Fig. 4D). By E17.5, wild-type TCAs had formed a thin fasciculus in the dorsal thalamus and prethalamus including TRN, which extended in parallel, orienting ventrolaterally (Fig. 4E). By contrast, *Olig2-KO* netrin G1+ fibers formed an abnormally thick fasciculus and extended randomly in the dorsal thalamus (Fig. 4F, arrowheads). These observations indicate that, in the *Olig2-KO* diencephalon, the initial changes in prethalamus/TE regionalization are followed by later disorganized axonal fasciculation and extension (Fig. 4G).

Retarded and disorganized thalamocortical projection in the *Olig2-KO* forebrain

The *Olig2-KO* mouse prethalamus shows defects as early as E10.5, before the onset of TCA formation, suggesting that the initial stage of projection formation would be disorganized in *Olig2-KO* mice. We thus examined TCA at E13.5 using DiI axonal tracing. DiI-labeled TCAs were observed, orienting dorsolaterally in the ventral telencephalon of wild-type animals (Fig. 5A). By contrast, in *Olig2-KO* mice, DiI-labeled TCAs had just crossed the telencephalon-diencephalon boundary (TDB), and had not yet reached the lateral ganglionic eminence (Fig. 5B). Measuring the length of the TCAs in the ventral telencephalon between the growing tip and the TDB, *Olig2-KO* TCAs were much shorter (around 60% reduction) than those of wild-type animals (Fig. 5C). The result clearly shows a reduction of TCA extension at early stages in the absence of Olig2 (Fig. 5A,B, insets).

We further examined whether TCAs reach the cerebral cortex and whether topographic thalamocortical projection is formed in the *Olig2-KO* mouse. DiI was injected into the middle part of the E18.5 cortex, and DiA was injected into the frontal and occipital poles of the same brain (Fig. 6A,B, insets). The frontal cortex had a connection with the medial part of the thalamus, the middle part with the central part, and occipital cortex with the lateral part in both normal control and *Olig2-KO* mice (Fig. 6C,D). Therefore, the topography of the reciprocal projection was roughly preserved in the absence of Olig2. However, axon arrangement was markedly disorganized in the *Olig2-KO* thalamus: whereas axons were arranged in parallel in the wild-type thalamus, those in *Olig2-KO* formed a thick fasciculus and crossed each other with abnormal overlapping course of axons (Fig. 6C-F). On closer examination, retrogradely labeled cell bodies were observed in the *Olig2-KO* dorsal thalamus (Fig. 6F, arrows), indicating that TCAs in *Olig2-KO* reached the cerebral cortex in spite of the initial delay of their extension.

Disorganized TCAs extend from non-Olig2 lineage cells

Olig2 is strongly expressed in the VZ of the prethalamus and weakly in the caudoventral part of the dorsal thalamus, whereas TCAs have defects of axon extension; therefore, we examined whether the axonal extension defect in the *Olig2-KO* dorsal thalamus is induced in a cell-autonomous or a non-cell-autonomous manner. If TCA defects in *Olig2-KO* mice are induced in a cell-autonomous manner, they should be shown by Olig2 lineage neurons. To analyze this, we again used *Olig2-KO*;Rosa26^{GFP} mice, and tamoxifen was administered to pregnant mice at E11.5 and/or E12.5 to label Olig2+ cells. At E13.5, when NF-M+ axons were disorganized in the lateral part of the dorsal thalamus of *Olig2-KO*;Rosa26^{GFP} mouse, axon aggregates were found in the nucleus-free zones (supplementary material Fig. S6A,B, arrows). Nevertheless, processes of GFP+ Olig2-lineage cells were present in the prethalamus showing radial extension, but were not present in cell-free zones (supplementary material Fig. S6C,D, asterisks). At E17.5, GFP+ axons of *Olig2-KO*;Rosa26^{GFP} mice were observed in the TRN, whereas no GFP+ axons were present in the dorsal thalamus (supplementary material Fig. S6E). Abnormally oriented axons extending randomly were GFP negative (supplementary material Fig. S6F, arrowheads). These results indicated that axons showing disorganized elongation do not belong to Olig2 lineage neurons, suggesting non-cell autonomous defect of axonal extension in the *Olig2-KO* dorsal thalamus.

Altered expression of axon guidance molecules in the *Olig2-KO* prethalamus

As axon arrangement was impaired in the *Olig2-KO* mouse dorsal thalamus, and axonal disorganization occurred in a non-cell-autonomous manner, it is highly probable that the expressions of axon guidance molecules are altered in the terrain through which

Development (2014) 141, 2075-2084 doi:10.1242/dev.097790

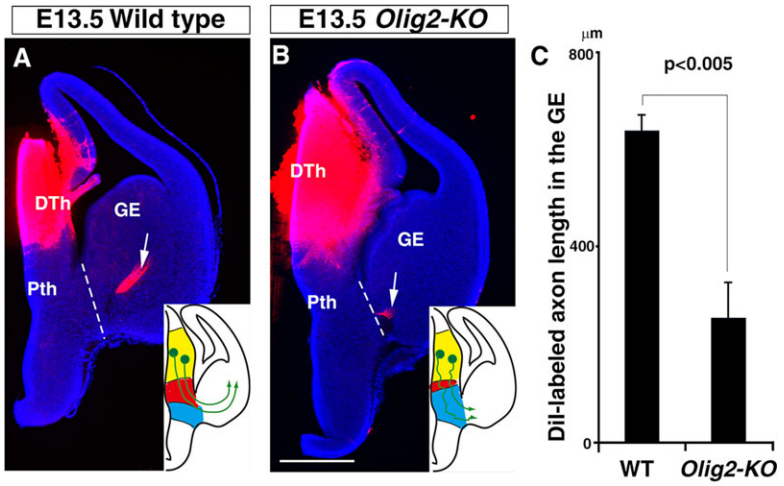

Fig. 5. Arrest of TCA extension at the initial stage of projection formation. (A,B) E13.5 forebrain with DiI crystal injection into the dorsal thalamus. Broken lines indicate the telencephalon-diencephalon boundary (TDB). Labeled TCAs had reached the lateral ganglionic eminence of the ventral telencephalon in the wild-type animal (arrow in A) whereas those in the *Olig2-KO* mouse had just crossed the TDB in the ventral telencephalon (arrow in B). DTh, dorsal thalamus; GE, ganglionic eminence; Pth, prethalamu. Insets show schematics of diencephalon regionalization and TCA extension. Scale bar: 500 μm. (C) Mean distance between the distal tip of DiI-labeled fibers and the TDB. Data are mean±s.e.m. (wild type, *n*=3; *Olig2-KO*, *n*=3; Student's *t*-test)

TCAs pass, including the prethalamus and the TE. We therefore conducted a microarray analysis for changes in the gene expression of axon guidance molecules in the diencephalon or basal forebrain comparing the transcriptomes of wild-type and *Olig2-KO* mice at E13.5 (Table 1). Efna, Epha and Sema genes, and *Unc5c* were shown to change their expression in the absence of Olig2. Using Allen Institute for Brain Science Web *in situ* hybridization data (http://developingmouse.brain-map.org/), we confirmed that *Epha3* and *Epha5* were expressed in the E13.5 diencephalon. We then examined the expression pattern of these molecules in the *Olig2-KO* diencephalon by *in situ* hybridization. In the E13.5 wild-type forebrain, the prethalamus is devoid of mRNA for *Epha3* and *Epha5*, and the Ephas-negative region continues to the TDB (Fig. 7A,C, asterisks), and both *Epha3* and *Epha5* are expressed in the TE (Fig. 7A,C; supplementary material Fig. S7A,C,E,G,I,K,M,O; Kudo et al., 2005). In the age-matched *Olig2-KO* forebrain, the *Epha3*- and *Epha5*-expressing TE was dorsally expanded and, conversely, the Ephas-negative prethalamus were reduced in size (Fig. 7B,D; supplementary material Fig. S7B,D,F,H,J,L,N,P). Thus, malformed formation of the prethalamus and TE was accompanied with the altered expression of axon guidance molecules, likely leading to the altered extension of TCAs. EphrinA5 (*Efna5*), which encodes one of the ligands for EphA3, was expressed in the dorsal thalamus, which seemed to be unchanged in the absence of Olig2 (Fig. 7E,F).

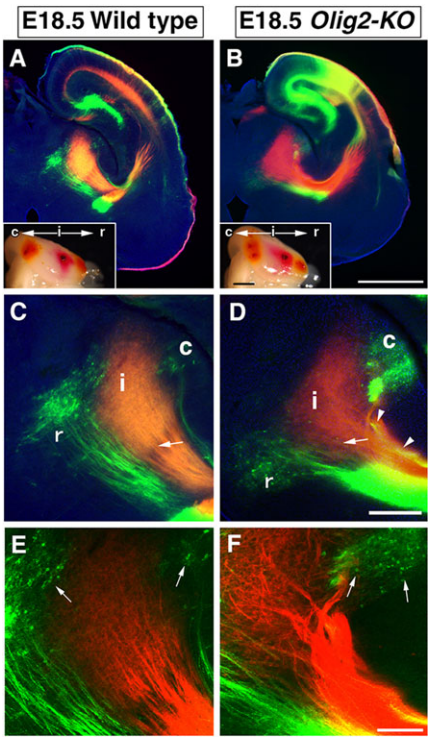

Fig. 6. Axonal tracing of reciprocal connection between the thalamus and cortex at E18.5. (A,B) Low-magnification pictures. Insets show injection sites of DiI (i, intermediate) and DiA (r, rostral; c, caudal). (C,D) Higher magnification pictures of the dorsal thalamus. c, i, r of the thalamus represent connections from c, i, r, respectively, of the cortical injection site. Arrows in C and D indicate positions of the external medullary laminae. Arrowheads in D indicate abnormal overlapping course of axons showing yellow color. (E,F) Laser scanning confocal micrographs. Arrows indicate retrogradely labeled cell bodies. Axons in the wild type are arranged in parallel (E), whereas those in *Olig2-KO* cross each other (F). Scale bars: 1 mm in B and inset; 200 μm in D; 100 μm in F.

Sema5a and *Unc5c* also showed changed expression in microarray analysis (Table 1); however, *in situ* hybridization analysis demonstrated that the expression patterns of *Sema5a* and *Unc5c* were not altered in the E13.5 diencephalon of *Olig2-KO* mice (not shown).

EphA3 suppresses axonal extension from cultured thalamic neurons

The above results strongly suggest that EphA3 and EphA5 are candidate molecules affecting the initial extension of TCAs. We next examined the roles of EphA3 in the neurite extension of dorsal thalamic neurons *in vitro*. Dissociated dorsal thalamic progenitor cells were cultured on the substrate double coated with PLL and either EphA3-Fc chimeric protein or human Fc for 40 h. Neurons were identified with class-III β tubulin immunohistochemistry (Fig. 8A,B). Neurite length on Fc-coated substrate was slightly but definitely different from that on EphA3 (33.3±2.38 μm and 24.4±2.90 μm, respectively, mean±s.e.m.) (Fig. 8C); thus, substrate-bound EphA3 apparently inhibited neurite extension from dorsal thalamic neurons.

Ectopic Olig2 does not affect EphA3 expression

We then examined whether Olig2 affects or suppresses EphA3 expression. In this experiment, we used a chick embryo neural tube, because gene expression hierarchy is well known in this region of the chick embryo (Liu et al., 2007; Mizuguchi et al., 2001) when compared with the fetal mouse diencephalon. *Epha3* expression in the

Development (2014) 141, 2075-2084 doi:10.1242/dev.097790

Table 1. Microarray expression analysis of control versus *Olig2-KO* brains at E13.5

Gene name	Gene symbol	RefSeq transcript ID	Probe set ID	FcOlig2/wild type	*P* value
Ephrin A1	*Efna1*	NM_001162425 /NM_010107	1416895_at	1.37	0.01
Ephrin B1	*Efnb1*	NM_010110	1418286_a_at	1.46	0.00
Ephrin B2	*Efnb2*	NM_010111	1449549_at	1.75	0.02
Ephrin B2	*Efnb2*		1419639_at	1.40	0.03
Eph receptor A3	*Epha3*	NM_010140	1426057_a_at	1.95	0.00
Eph receptor A3	*Epha3*		1425574_at	1.59	0.00
Eph receptor A3	*Epha3*		1455426_at	1.35	0.00
Eph receptor A3	*Epha3*		1425575_at	1.29	0.01
Eph receptor A5	*Epha5*	NM_007937	1420557_at	1.67	0.01
Eph receptor A5	*Epha5*		1435286_at	1.12	0.04
Semaphorin 3E	*Sema3e*	NM_011348	1442226_at	1.56	0.00
Semaphorin 4B	*Sema4b*	NM_013659	1455678_at	1.41	0.03
Semaphorin 5A	*Sema5a*	NM_009154	1437422_at	0.61	0.01
UNC-5 homolog C	*Unc5c*	NM_009472	1449522_at	0.79	0.01

Significant changes were observed in genes encoding these axon guidance molecules.

normal E6 chick spinal cord was observed in the ventral VZ and ventral horn (VH). In the VZ, *Epha3* expression was partially overlapped with Olig2, whereas motoneurons in the ventral horn, which are of Olig2 lineage, do not express Olig2. Olig2 was transfected to the E3 chick neural tube and E6 spinal cord was examined with GFP, Olig2, Islet1/2 and HB9 immunohistochemistry, and *Epha3 in situ* hybridization. Olig2 was overexpressed on the electroporated side (supplementary material Fig. S8A,B), which induced ectopic Islet1/2 but did not induce HB9 (not shown). Signal intensity of *Epha3* expressed in the VZ and VH was measured with ImageJ software, and the ratio of electroporated side/non-electroporated side was calculated and compared between Olig2-transfected and GFP-transfected samples. Signal intensity was not changed after Olig2 or EGFP transfection in both VZ and the ventral horn (supplementary material Fig. S8F). The ratio was 0.94-1.01 and was not statistically significant. The results indicate that ectopic overexpression of Olig2 does not affect *Epha3* expression.

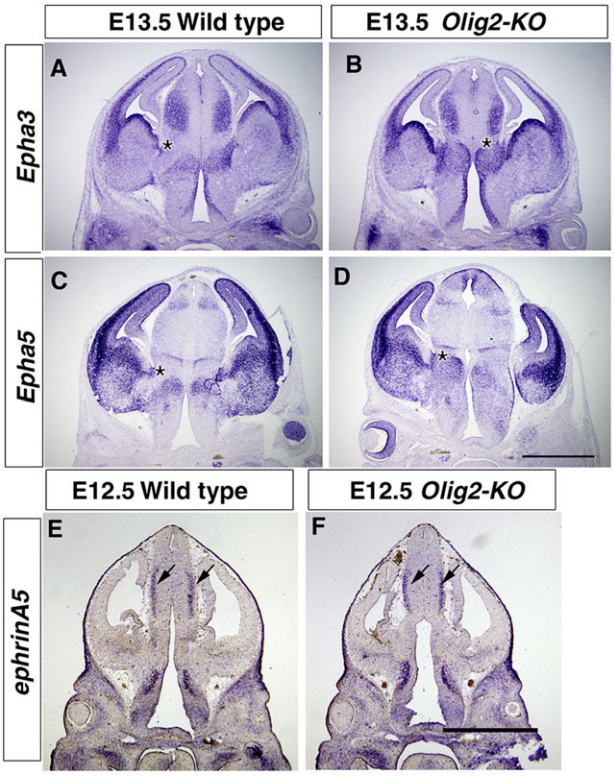

Fig. 7. Altered expression of *Epha3* and *Epha5* in the E13.5 *Olig2-KO* mouse diencephalon. (A,B) *Epha3 in situ* hybridization. (C,D) *Epha5 in situ* hybridization. Note that an Ephas-negative area is observed in the control prethalamus, being intercalated between the dorsal thalamus and the ventral telencephalon (asterisks in A and C). By contrast, the Ephas-negative area is very narrow in the *Olig2-KO* diencephalon (asterisks in B and D). (E,F) EphrinA5 (*Efna5*) *in situ* hybridization. EphrinA5 is expressed in both the wild-type and *Olig2-KO* dorsal thalamus (arrows). Scale bars: 1 mm.

DISCUSSION

In the present study, the *Olig2-KO* mouse diencephalon was examined morphologically, and we found malformation of the prethalamus and TE, followed by disorganized extension of TCAs. These results indicate that Olig2 controls proper formation of the prethalamus and also that proper formation of the prethalamus controls the initial extension of TCAs. Together, our results provide possible molecular mechanisms underlying initial TCA extension in the prethalamus.

Olig2 regulates proper formation of the prethalamus

Olig2 is expressed in VZ cells of the prethalamus, which develops into TRN and the zona incerta (Inamura et al., 2011), which are mostly composed of GABAergic neurons (Ottersen and Storm-Mathisen, 1984). We previously demonstrated that distribution of GABAergic neurons is nearly normal in the *Olig2-KO* forebrain compared with normal control animals (Ono et al., 2008), and a fate-mapping study demonstrated that Olig2 lineage cells differentiate into GABAergic neurons in the absence of Olig2 (Takebayashi et al., 2008). In the present study, we examined the formation of the prethalamus at much younger stages: E10.5-E13.5. The *Dlx2*-positive, as well as *Lhx5*-negative, prethalamus in *Olig2-KO* mice was markedly reduced in size (Figs 1, 2). Accompanying the size reduction of the prethalamus, the TE expanded dorsally. The reduced size of the prethalamus is probably caused both by elevated apoptosis at E10.5 (supplementary material Fig. S2) and by the fate change of Olig2 lineage cells from prethalamus cells to TE cells (Fig. 3; supplementary material Fig. S4). It is noteworthy that this is the first demonstration of Olig2 function in early forebrain patterning beyond its known role in glial development (Cai et al., 2007; Lu et al., 2002; Ono et al., 2008, 2009). We previously

Development (2014) 141, 2075-2084 doi:10.1242/dev.097790

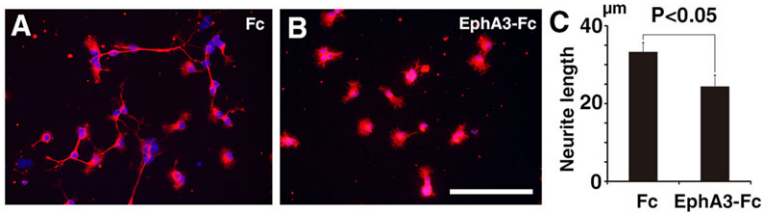

Fig. 8. Suppression of neurite extension from cultured thalamic neurons by EphA3. (A,B) Dissociated thalamus progenitor cells were cultured on substrate double-coated with poly-L-lysine and with human Fc (A) or mouse EphA3-human Fc (B) chimeric protein. Cultured cells were stained with class-III β tubulin immunohistochemistry (red). (C) Neurite extension was apparently impaired on substrate coated with EphA3. *n*=3 independent cultures. Scale bar: 100 μm in B.

reported that loss of Olig2 does not affect apoptosis in the pMN domain (Takebayashi et al., 2008). Other parts of the E10.5 forebrain regions, such as the *Dlx2*-positive ganglionic eminence or (*Dlx2*-negative) cerebral cortex, revealed a similar level of apoptosis (not shown). Therefore, involvement of Olig2 in the apoptotic pathway might be dependent on the stage or region of the central nervous system. In addition, it is probable that Olig2 interacts with other transcription factors, such as Tbr2, for proper boundary formation in the TE, as has been reported in the developing neural tube (Helms and Johnson, 2003). Further studies are necessary to clarify the mechanisms of Olig2 function in forebrain patterning.

Proper formation of the prethalamus and TE is required for early thalamocortical projection

Another important new finding is that loss of Olig2 results in retardation of initial TCA extension, which leads to abnormal fasciculation and random orientation of TCA at the late fetal stage (Figs 4-6). It is highly probable that the delay of TCA extension is caused by reduction of prethalamus formation and expansion of the TE, both of which are induced by loss of Olig2: (1) the prethalamus occupies an exit region for TCAs; (2) a defect in the thalamocortical projection was probably induced in a non-cell-autonomous manner (see supplementary material Fig. S6); (3) EphA3 and EphA5 expression is observed in the TE but not in the prethalamus; (4) EphA3 and EphA5 expression occupies the route of TCA extension in the *Olig2-KO* diencephalon (Fig. 7; supplementary material Fig. S7); (5) ephrinA5, a possible counterpart molecule of EphA3, is expressed in the dorsal thalamus; (6) substrate-bound EphA3 suppresses neurite extension from thalamic neurons *in vitro* (Fig. 8). Eph receptors and ephrin ligands act as a repellant molecule system in neural circuit formation. In addition, ephrin A proteins also recognize and transduce the reverse signaling of EphA proteins, which also includes axon repulsion (Rashid et al., 2005; Xu and Henkemeyer, 2012). Together, these observations suggest that the *Epha3*- and *Epha5*-negative prethalamus may provide a permissive or less inhibitory substrate for TCAs, and that occupation of *Epha3* and *Epha5* in the exit route impairs initial extension of TCAs in the *Olig2-KO* diencephalon. It is probable that EphA3 negatively regulates TCA elongation, and, therefore, expansion of Ephas-positive TE may impair initial TCA extension in the *Olig2-KO* forebrain (Figs 4, 5).

Another possible functional role of the prethalamus in TCA extension is contact guidance of prethalamic axons to TCAs. Mitrofanis and Baker (Mitrofanis and Baker, 1993) proposed that pioneer fibers from the prethalamus extending into the thalamus guide TCAs to the prethalamus. Our observation might support the possible association of thalamic and prethalamic axons as these axons do not express a combination of repellant molecules; while thalamic axons may express ephrinA5, its counterpart molecules EphA3 and EphA5 are not expressed in prethalamic axons (Fig. 7). It remains unknown whether these axons express molecules that mediate contact attraction.

The *Olig2-KO* forebrain includes other minor defects. For example, the prethalamus region at E11.5 and E12.5 was constricted in *Olig2-KO* mice (Fig. 1, Fig. 7E,F). This constriction was, however, partially recovered by E13.5 (Figs 2, 3, Fig. 7A-D) [probably owing to elevated proliferation in the *Olig2-KO* prethalamus (supplementary material Fig. S2H)], and cytoarchitecture, such as radial arrangement of the prethalamic cells and radial fiber extension, was preserved normally in the absence of Olig2 (Fig. 3D; supplementary material Fig. S6). Therefore, the constriction of the prethalamus at early stages may not be the cause of the retardation of TCAs in the *Olig2-KO* forebrain, although this possibility cannot be ruled out completely. In addition, the dorsal thalamus of the *Olig2-KO* mouse shows slight hypoplasia (supplementary material Fig. S3K), and the EphA3-positive region is also slightly reduced in the *Olig2-KO* thalamus (Fig. 7). We could not clarify whether the slight reduction of EphA3 expression in the dorsal thalamus affects the initial delay of TCA extension. However, as EphA3 negatively regulates TCA extension, reduction of EphA3 expression might not have a strong effect on the initial delay of axon elongation. As hypoplasia of the prethalamus is the severest defect within the *Olig2-KO* diencephalon, it is the most likely cause of the initial retardation and impairment of TCA guidance.

The prethalamus and TE have been supposed to be intermediate targets for formation of the thalamocortical projection, as loss of transcription factors expressed in these regions induces defects of thalamocortical projection, which includes Pax6, Mash1 (Ascl1 – Mouse Genome Informatics), Tbr1 (López-Bendito and Molnár, 2003), Dlx1/2 and Ebf1 (Garel et al., 2002) and Olig2 (present study). Transcription factors regulate region identity in the rostral-caudal axis (Kiecker and Lumsden, 2004; Puelles and Rubenstein, 2003; Rubenstein et al., 1998) and cell-fate determination in the dorsoventral axis (Helms and Johnson, 2003; Tanabe and Jessell, 1996). Recently, evidence has supported that transcription factors regulating cell-type specification also regulate cell migration and neural circuit formation (Chédotal and Rijli, 2009; Shirasaki et al., 2006). Cell-fate determination may include the cell-type-specific behavior of committed cells through regulation of the expression of cytoskeletal molecules and receptors for axon guidance molecules.

In our observations, prethalamus formation is controlled by Olig2, which leads to EphA3- and EphA5-negative terrain for the initial extension of TCAs; therefore, transcription factors also control the milieu or environment for axon elongation, regulating neural circuit formation indirectly. As Olig2 may not suppress or regulate EphA3 expression directly (supplementary material Fig. S8) and as the expression of morphogen molecules that may affect EphA3 expression was not altered in the *Olig2-KO* diencephalon (supplementary material Fig. S3D,E,I,J), it is probable that putative programs for TE formation regulate EphA3 expression. Olig2 is involved in multistep processes of diencephalon formation and may indirectly repress EphA3 expression through interacting with transcription factors involved in TE development.

In conclusion, the present study elucidates that Olig2 is crucial for proper formation of the prethalamus, especially the boundary between the prethalamus and TE, and that proper formation of the prethalamus is crucial for correct extension of TCAs. Therefore,

Development (2014) 141, 2075-2084 doi:10.1242/dev.097790

appropriate regionalization of the prethalamus and TE provides a pathway from the dorsal thalamus to the ventral telencephalon.

MATERIALS AND METHODS

Animals and tissue preparation

The animals used in this study were Olig2^{KICreER} (Takebayashi et al., 2002b), *Olig2*$^{-/-}$ (Lu et al., 2002), ROSA26-GAP43-EGFP (Nakahira et al., 2006) and wild-type ICR mice (Slc, Shizuoka, Japan). Genotyping was performed as described previously (Takebayashi et al., 2002b; Tatsumi et al., 2008). Fertilized chick eggs were purchased from Yamagishi Corporation (Mie, Japan) and were incubated at 37°C. Embryonic stages of chicks were determined according to Hamburger and Hamilton (Hamburger and Hamilton, 1951). At least three independent experiments were carried out in all histological and culture analyses, including DiI tracing. All animal procedures were approved by the Animal Research Committee of Kyoto Prefectural University of Medicine and of the National Institute for Physiological Sciences.

To obtain *Olig2-KO* mice, Olig2^{KICreER} heterozygous mice were mated and the day when the vaginal plug was found was regarded as embryonic day 0.5 (E0.5). To label Olig2 lineage cells, Olig2^{KICreER};ROSA26-GAP43-EGFP double heterozygous mice were mated, and tamoxifen (TM; 3 mg/animal) was injected intraperitoneally into pregnant mothers with fetuses at E10.5, E11.5 or E11.5 and E12.5, as described previously (Masahira et al., 2006). Pregnant mice were deeply anesthetized with pentobarbital (100 mg/kg body weight), and fetal mice were removed from the uterus. Fetal mouse brains were fixed with 4% paraformaldehyde (PFA) in PBS overnight, and subsequently with 20% sucrose in PBS. Fixed brains were cut coronally with a cryostat at 20 µm, and sections were thaw-mounted onto MAS-coated glass slides (Matsunami Glass, Tokyo, Japan).

In situ hybridization

In situ hybridization was performed using digoxygenin-labeled antisense riboprobes, as described previously (Ding et al., 2005; Wilkinson, 1998). cDNAs used in this study were as follows: *mDlx2* (NM_010054, nt_746-1355), *mephrinA5* (NM_207654, nt204-831), *mUuc5c* (Watanabe et al., 2006), *mEpha3* (NM_010140, nt_2760-3340), *mEpha5* (NM_007937, nt_1135-2100), *mFgf8* (Ohuchi et al., 1994), *mOlig3* (Takebayashi et al., 2002a), *mLhx5* (Hirata et al., 2006), *mShh* (Iseki et al., 1996), *mSema5a* (NM_009154, nt_634-1162) and chick *EphA3* (Iwamasa et al., 1999). Sense probes were used as a negative control, which did not show specific signals.

Immunohistochemistry

Immunohistochemistry was carried out as previously described (Ono et al., 2004, 2008). The GFP signal in the Rosa26-GAP43-EGFP reporter mouse brain was enhanced by incubation with fluorescein-conjugated tyramide (Tyramide Signal Amplification-Fluorescein Systems; PerkinElmer Life Science, Boston, MA, USA). Primary antibodies used were: rabbit anti-Olig2 (1:1000, AB9610; Millipore, Temecula, CA, USA; 1:500, 0B-905; IBL, Takasaki, Japan), rabbit anti-GFP (1:1000, AB3080; Millipore), rat anti-GFP (1:1000, 04404-84; Nacalai Tesque, Kyoto, Japan), rabbit anti-calretinin (1:1000, 7697; Swant, Marly, Switzerland), rabbit anti-Tbr1 (1:500, ab31940; Abcam, Cambridge, UK), rabbit anti-Tbr2 (1:500, ab23345; Abcam), mouse anti-Islet1/2 (4D5, 1:50; DSHB), mouse anti-neurofilament M (Watanabe et al., 2006), mouse anti-netrin G1 (1:500; Niimi et al., 2007), rabbit anti-netrin G1 (1:10; Niimi et al., 2007), mouse anti-HB9 (1:50, 5C10; DSHB), rabbit anti-cleaved caspase 3 (1:500, 9661; Cell Signaling, Danvers, MA), rabbit anti-Cre (1:1000, 69050-3; Novagen, San Diego, CA) and rabbit anti-phospho-histone H3 (pH3; 1:500, 06-570; Millipore). Stained sections were observed under a bright field and epifluorescent microscope (BX-51; Olympus, Tokyo, Japan), and images were captured via a CCD camera (DP-71; Olympus).

Axonal tracing with lipophilic carbocyanine dye

In order to label early TCAs in the E13.5 brain, crystals of lipophilic dye DiI (1,1′-dioctadecyl-3,3,3′,3′-tetramethylindocarbocyanine perchlorate; Invitrogen, Eugene, OR, USA) were applied to the dorsal thalamus of wild-type and *Olig2-KO* animals after fixation. Tissues were kept in 4% PFA at 37°C for 4 days. To label reciprocal connections between the dorsal thalamus and cortex in the E17.5 and E18.5 cortex, 2% solutions of DiI and DiA [4-(4-(dihexadecylamino)styryl)-N-methylpyridinium iodide; Invitrogen] were used as tracers. DiA was injected into the frontal and occipital poles, and DiI was injected into the middle part of the cortex (Fig. 6A,B, insets). They were kept at 37°C in the fixative for 2 weeks and then cut coronally with a vibratome at 100 µm. Sections were stained with Hoechst33342, and observed under an epifluorescent microscope and a confocal laser scanning microscope (FV-1000; Olympus).

Microarray preparation, processing and statistical analysis

The samples were grouped into two sample types: *Olig2-KO* (Lu et al., 2002) and the wild type. RNA was purified from the E13.5 ventral forebrain from *Olig2-KO* (*Olig2*$^{-/-}$) and the wild type (*Olig2*$^{+/+}$). RNA samples were prepared by pooling RNAs extracted from three brains to constitute one replicate and each sample type was prepared in five replicates. cRNA hybridization probes were hybridized to Affymetrix Mouse Whole Genome MOE430 2.0 arrays. The R-CRAN statistical language and Bioconductor software package (Gentleman et al., 2004) were used throughout the expression analyses. Raw image files were processed using Affymetrix GCOS and the Microarray Suite (MAS) 5.0 algorithm. The probe signal levels were quantile normalized, summarized and then transformed to the log 2 expression using GCRMA (gcrma R-package; Irizarry et al., 2003) and Frozen RMA (fRMA package; McCall and Irizarry, 2011). Gene filtering was performed using the Wilcoxon signed-rank test to select probe sets that were 'consistently expressed' (P<0.04) in at least one group (mas5calls R-package; Bioconductor). All samples showed good quality control according to MAS5.0 guidelines and the AffyQC report (R-package; Bioconductor). Principal component analysis (PCA) was used to reduce the dimensionality of the whole dataset and measure the degree of similarity between samples (dudi.pca R-package; Thioulouse and Dray, 2007). We had to withdraw two replicates from each sample type as they were aberrant. The subsequent three-dimensional PCA plot confirmed a high degree of similarity among samples of the same sample type and much less similarity among samples of different sample types. We used LIMMA statistical analysis (Smyt, 2004) to determine the differentially expressed genes in *Olig2-KO*. The resulting P-values were adjusted to FDR <5% with the Benjamini-Hochberg method to control the mean proportion of false positives (q-value R-package; Storey and Tibshirani, 2003) and a kernel-based FDR method to assess the probability of being false positive for a specific gene (kerfdr R-package; Guedj et al., 2009). Microarray data have been deposited in Gene Expression Omnibus with accession number GSE56389.

Dissociation culture of dorsal thalamus neurons

The dorsal thalamus at E12.5 was dissected free from the fetal brain, minced into small pieces, treated with 0.1% trypsin for 15 min at 37°C, and then triturated with a fire-polished pasture pipette. Dissociated cell suspension (1×10^5 cells/ml) was prepared in culture medium (MEM containing 5% fetal bovine serum and 5% horse serum). For analyses of the substrate-bound form of EphA3, plastic dishes (35 mm in diameter) were sequentially coated with poly-L lysine (PLL, 80 µg/ml; Sigma, St Louis, MO, USA) overnight at 4°C and then with mouse EphA3-human Fc or human Fc (100 nM; R&D Systems, Minneapolis, MN, USA) for 5 h at 37°C. After rinsing the culture substrates with PBS, 2 ml thalamic cell suspension was plated onto the culture dishes. Cultures were maintained for 40 h. They were fixed with 4% PFA and stained with anti-class III β tubulin antibody (1:1000, G7121; Promega) to examine neurite extension. Three independent culture experiments were performed. In each experiment, epifluorescent photomicrographs were taken of 9-15 randomly chosen fields and the length of neurites with more than 50 labeled cells was measured with ImageJ software (NIH).

Electroporation

In ovo electroporation was performed as previously described (Ono et al., 2004). E3 chick embryos (HH stage 17-20; Hamburger and Hamilton, 1951) were used. DNA of pCAGGS-EGFP (Gotoh et al., 2011) solution with or

Development (2014) 141, 2075-2084 doi:10.1242/dev.097790

without pCAGGS-mOlig2 (Mizuguchi et al., 2001) was injected into the central canal, and square pulses (30 V, 50 ms, twice; Nihon Koden, SEN-3401) were delivered to the embryos. The embryos were fixed at E6 (HH stage 27-29) and analyzed histologically. Gene expression was analyzed as the ratio of signal intensity between the electroporated side and non-electroporated side, and the ratio of Olig2-transfected samples was compared with that of EGFP-transfected samples.

Image analysis

The area of the *Dlx2+* region and neurite length both *in vivo* and *in vitro* was measured with ImageJ software after images were captured with a CCD camera as above. In all cases, quantitative analysis was carried out using at least three *Olig2-KO* or wild-type/heterozygous mice.

Acknowledgements

Some monoclonal antibodies were obtained from DSHB. We thank Dr Martyn Goulding (The Salk Institute) for providing the reporter mouse, and Drs Hideaki Tanaka (Kumamoto University), Hideyo Ohuchi (Okayama University), Masahiko Hibi (Nagoya University), Jun-ichi Miyazaki (Osaka University) and Kazunori Nakajima (Keio University) for cDNAs and helpful comments.

Competing interests

The authors declare no competing financial interests.

Author contributions

The project was designed by K.O., H.T., K.S. and K.I. Histological and culture experiments were performed by K.O., A.C., T.N., H.G., A.U., O.A., Q.Z. and S.I., and microarray analysis was carried out by A.C., C.M.P. and O.A. The manuscript was written by K.O. and H.T. with the remaining authors commenting on the manuscript.

Funding

This work was supported by Grants-in-Aid for Scientific Research (C) and an Innovated Area (Neural Diversity and Neocortical Organization) provided by JSPS and MEXT, Japan (to K.O.); by the Cooperative Study Program of NIPS (to K.O., H.T., H.G. and K.I.); by Kumamoto University (K.O., H.T., H.G. and K.S.); by FIRST program (to S.I.); by ARSEP scholarships (A.C.); and by Institut National de la Santé et de la Recherche Médicale and the program 'Investissements d'Avenir' [ANR-1-IAIHU-06] (C.M.P).

Supplementary material

Supplementary material available online at
http://dev.biologists.org/lookup/suppl/doi:10.1242/dev.097790/-/DC1

References

Abbott, L. C. and Jacobowitz, D. M. (1999). Developmental expression of calretinin-immunoreactivity in the thalamic eminence of the fetal mouse. *Int. J. Dev. Neurosci.* **17**, 331-345.

Braisted, J. E., Catalano, S. M., Stimac, R., Kennedy, T. E., Tessier-Lavigne, M., Shatz, C. J. and O'Leary, D. M. (2000). Netrin-1 promotes thalamic axon growth and is required for proper development of the thalamocortical projection. *J. Neurosci.* **20**, 5792-5801.

Braisted, J. E., Ringstedt, T. and O'Leary, D. D. M. (2009). Slits are chemorepellents endogenous to hypothalamus and steer thalamocortical axons into ventral telencephalon. *Cereb. Cortex* **19** Suppl. 1, i144-i151.

Bulfone, A., Puelles, L., Porteus, M. H., Frohman, M. A., Martin, G. R. and Rubenstein, J. L. (1993). Spatially restricted expression of Dlx-1, Dlx-2 (Tes-1), Gbx-2, and Wnt-3 in the embryonic day 12.5 mouse forebrain defines potential transverse and longitudinal segmental boundaries. *J. Neurosci.* **13**, 3155-3172.

Bulfone, A., Smiga, S. M., Shimamura, K., Peterson, A., Puelles, L. and Rubenstein, J. L. R. (1995). T-Brain-1: a homolog of Brachyury whose expression defines molecularly distinct domains within the cerebral cortex. *Neuron* **15**, 63-78.

Cai, J., Chen, Y., Cai, W.-H., Hurlock, E. C., Wu, H., Kernie, S. G., Parada, L. F. and Lu, Q. R. (2007). A crucial role for Olig2 in white matter astrocyte development. *Development* **134**, 1887-1899.

Chédotal, A. and Rijli, F. M. (2009). Transcriptional regulation of tangential neuronal migration in the developing forebrain. *Curr. Opin. Neurobiol.* **19**, 139-145.

Deng, J. and Elberger, A. J. (2003). Corticothalamic and thalamocortical pathfinding in the mouse: dependence on intermediate targets and guidance axis. *Anat. Embryol.* **207**, 177-192.

Ding, L., Takebayashi, H., Watanabe, K., Ohtsuki, T., Tanaka, K. F., Nabeshima, Y.-i., Chisaka, O., Ikenaka, K. and Ono, K. (2005). Short-term lineage analysis of dorsally derived Olig3 cells in the developing spinal cord. *Dev. Dyn.* **234**, 622-632.

Dufour, A., Seibt, J., Passante, L., Depaepe, V., Ciossek, T., Frisén, J., Kullander, K., Flanagan, J. G., Polleux, F. and Vanderhaeghen, P. (2003). Area specificity and topography of thalamocortical projections are controlled by ephrin/Eph genes. *Neuron* **39**, 453-465.

Garel, S., Yun, K., Grosschedl, R. and Rubenstein, J. L. R. (2002). The early topography of thalamocortical projections is shifted in Ebf1 and Dlx1/2 mutant mice. *Development* **129**, 5621-5634.

Gentleman, R. C., Carey, V. J., Bates, D. M., Bolstad, B., Dettling, M., Dudoit, S., Ellis, B., Gautier, L., Ge, Y. C., Gentry, J. et al. (2004). Bioconductor: open software development for computational biology and bioinformatics. *Genome Biol.* **5**, R80.

Gotoh, H., Ono, K., Takebayashi, H., Harada, H., Nakamura, H. and Ikenaka, K. (2011). Genetically-defined lineage tracing of Nkx2.2-expressing cells in chick spinal cord. *Dev. Biol.* **349**, 504-511.

Guedj, M., Robin, S., Celisse, A. and Nuel, G. (2009). Kerfdr: a semi-parametric kernel-based approach to local false discovery rate estimation. *BMC Bioinformatics* **10**, 84.

Hamburger, V. and Hamilton, H. L. (1951). A series of normal stages in the development of the chick embryo. *J. Morphol.* **88**, 49-92.

Helms, A. W. and Johnson, J. E. (2003). Specification of dorsal spinal cord interneurons. *Curr. Opin. Neurobiol.* **13**, 42-49.

Hirata, T., Nakazawa, M., Muraoka, O., Nakayama, R., Suda, Y. and Hibi, M. (2006). Zinc-finger genes *Fez* and *Fez-like* function in the establishment of diencephalon subdivisions. *Development* **133**, 3993-4004.

Inamura, N., Ono, K., Takebayashi, H., Zalc, B. and Ikenaka, K. (2011). Olig2 lineage cells generate GABAergic neurons in the prethalamic nuclei, including the zona incerta, ventral lateral geniculate nucleus and reticular thalamic nucleus. *Dev. Neurosci.* **33**, 118-129.

Irizarry, R. A., Ooi, S. L., Wu, Z. and Boeke, J. D. (2003). Use of mixture models in a microarray-based screening procedure for detecting differentially represented yeast mutants. *Stat. Appl. Genet. Mol. Biol.* **2**, Article1.

Iseki, S., Araga, A., Ohuchi, H., Nohno, T., Yoshioka, H., Hayashi, F. and Noji, S. (1996). Sonic hedgehog is expressed in epithelial cells during development of whisker, hair, and tooth. *Biochem. Biophys. Res. Commun.* **218**, 688-693.

Iwamasa, H., Ohta, K., Yamada, T., Ushijima, K., Terasaki, H. and Tanaka, H. (1999). Expression of Eph receptor tyrosine kinases and their ligands in chick embryonic motor neurons and hindlimb muscles. *Dev. Growth Differ.* **41**, 685-698.

Kiecker, C. and Lumsden, A. (2004). Hedgehog signaling from the ZLI regulates diencephalic regional identity. *Nat. Neurosci.* **7**, 1242-1249.

Kudo, C., Ajioka, I., Hirata, Y. and Nakajima, K. (2005). Expression profiles of EphA3 at both the RNA and protein level in the developing mammalian forebrain. *J. Comp. Neurol.* **487**, 255-269.

Leyva-Díaz, E. and López-Bendito, G. (2013). In and out from the cortex: development of major forebrain connections. *Neuroscience* **254**, 26-44.

Liu, Z., Hu, X., Cai, J., Liu, B., Peng, X., Wegner, M. and Qiu, M. (2007). Induction of oligodendrocyte differentiation by Olig2 and Sox10: evidence for reciprocal interactions and dosage-dependent mechanisms. *Dev. Biol.* **302**, 683-693.

López-Bendito, G. and Molnár, Z. (2003). Thalamocortical development: how are we going to get there? *Nat. Rev. Neurosci.* **4**, 276-289.

López-Bendito, G., Cautinat, A., Sánchez, J. A., Bielle, F., Flames, N., Garratt, A. N., Talmage, D. A., Role, L. W., Charnay, P., Marín, O. and Garel, S. (2006). Tangential neuronal migration controls axon guidance: a role for neuregulin-1 in thalamocortical axon navigation. *Cell* **125**, 127-142.

Lu, Q. R., Sun, T., Zhu, Z., Ma, N., Garcia, M., Stiles, C. D. and Rowitch, D. H. (2002). Common developmental requirement for Olig function indicates a motor neuron/oligodendrocyte connection. *Cell* **109**, 75-86.

Masahira, N., Takebayashi, H., Ono, K., Watanabe, K., Ding, L., Furusho, M., Ogawa, Y., Nabeshima, Y.-i., Alvarez-Buylla, A., Shimizu, K. et al. (2006). Olig2-positive progenitors in the embryonic spinal cord give rise not only to motoneurons and oligodendrocytes, but also to a subset of astrocytes and ependymal cells. *Dev. Biol.* **293**, 358-369.

McCall, M. N. and Irizarry, R. A. (2011). Thawing frozen robust multi-array analysis (fRMA). *BMC Bioinformatics* **12**, 369.

Mitrofanis, J. and Baker, G. E. (1993). Development of the thalamic reticular and perireticular nuclei in rats and their relationship to the course of growing corticofugal and corticopetal axons. *J. Comp. Neurol.* **338**, 575-587.

Mizuguchi, R., Sugimori, M., Takebayashi, H., Kosako, H., Nagao, M., Yoshida, S., Nabeshima, Y.-i., Shimamura, K. and Nakafuku, M. (2001). Combinatorial roles of olig2 and neurogenin2 in the coordinated induction of pan-neuronal and subtype-specific properties of motoneurons. *Neuron* **31**, 757-771.

Molnár, Z., Garel, S., López-Bendito, G., Maness, P. and Price, D. J. (2012). Mechanisms controlling the guidance of thalamocortical axons through the embryonic forebrain. *Eur. J. Neurosci.* **35**, 1573-1585.

Nakahira, E., Kagawa, T., Shimizu, T., Goulding, M. D. and Ikenaka, K. (2006). Direct evidence that ventral forebrain cells migrate to the cortex and contribute to the generation of cortical myelinating oligodendrocytes. *Dev. Biol.* **291**, 123-131.

Nakashiba, T., Nishimura, S., Ikeda, T. and Itohara, S. (2002). Complementary expression and neurite outgrowth activity of netrin-G subfamily members. *Mech. Dev.* **111**, 47-60.
Niimi, K., Nishimura-Akiyoshi, S., Nakashiba, T. and Itohara, S. (2007). Monoclonal antibodies discriminating netrin-G1 and netrin-G2 neuronal pathways. *J. Neuroimmunol.* **192**, 99-104.
Ohuchi, H., Yoshioka, H., Tanaka, A., Kawakami, Y., Nohno, T. and Noji, S. (1994). Involvement of androgen-induced growth factor (FGF-8) gene in mouse embryogenesis and morphogenesis. *Biochem. Biophys. Res. Commun.* **204**, 882-888.
Ono, K., Yasui, Y. and Ikenaka, K. (2004). Lower rhombic lip-derived cells undergo transmedian tangential migration followed by radial migration in the chick embryo brainstem. *Eur. J. Neurosci.* **20**, 914-922.
Ono, K., Takebayashi, H., Ikeda, K., Furusho, M., Nishizawa, T., Watanabe, K. and Ikenaka, K. (2008). Regional- and Temporal-dependent changes in the differentiation of Olig2 progenitors in the forebrain, and the impact on astrocyte development in the dorsal pallium. *Dev. Biol.* **320**, 456-468.
Ono, K., Takebayashi, H. and Ikenaka, K. (2009). Olig2 transcription factor in the developing and injured forebrain; Cell lineage and glial development. *Mol. Cells* **27**, 397-401.
Ottersen, O. P. and Storm-Mathisen, J. (1984). GABA-containing neurons in the thalamus and pretectum of the rodent. An immunohistochemical study. *Anat. Embryol.* **170**, 197-207.
Puelles, L. (2001). Brain segmentation and forebrain development in amniotes. *Brain Res. Bull.* **55**, 695-710.
Puelles, L. and Rubenstein, J. L. R. (2003). Forebrain gene expression domains and the evolving prosomeric model. *Trends Neurosci.* **26**, 469-476.
Rashid, T., Upton, A. L., Blentic, A., Ciossek, T., Knöll, B., Thompson, I. D. and Drescher, U. (2005). Opposing gradients of ephrin-As and EphA7 in the superior colliculus are essential for topographic mapping in the mammalian visual system. *Neuron* **47**, 57-69.
Rubenstein, J. L. R., Shimamura, K., Martinez, S. and Puelles, L. (1998). Regionalization of the prosencephalic neural plate. *Annu. Rev. Neurosci.* **21**, 445-477.
Shirasaki, R., Lewcock, J. W., Littieri, K. and Pfaff, S. L. (2006). FGF as a target-derived chemoattractant for developing motor axons genetically programmed by the LIM code. *Neuron* **50**, 841-853.
Smyth, G. K. (2004). Linear models and empirical bayes methods for assessing differential expression in microarray experiments. *Stat. Appl. Genet. Mol. Biol.* **3**, Article3.
Storey, J. D. and Tibshirani, R. (2003). Statistical significance for genomewide studies. *Proc. Natl. Acad. Sci. U.S.A.* **100**, 9440-9445.
Takebayashi, H., Ohtsuki, T., Uchida, T., Kawamoto, S., Okubo, K., Ikenaka, K., Takeichi, M., Chisaka, O. and Nabeshima, Y.-i. (2002a). Non-overlapping expression of Olig3 and Olig2 in the embryonic neural tube. *Mech. Dev.* **113**, 169-174.
Takebayashi, H., Nabeshima, Y., Yoshida, S., Chisaka, O., Ikenaka, K. and Nabeshima, Y.-i. (2002b). The basic helix-loop-helix factor olig2 is essential for the development of motoneuron and oligodendrocyte lineages. *Curr. Biol.* **12**, 1157-1163.
Takebayashi, H., Usui, N., Ono, K. and Ikenaka, K. (2008). Tamoxifen modulates apoptosis in multiple modes of action in CreER mice. *Genesis* **46**, 775-781.
Tanabe, Y. and Jessell, T. M. (1996). Diversity and pattern in the developing spinal cord. *Science* **274**, 1115-1123.
Tatsumi, K., Takebayashi, H., Manabe, T., Tanaka, K. F., Makinodan, M., Yamauchi, T., Makinodan, E., Matsuyoshi, H., Okuda, H., Ikenaka, K. et al. (2008). Genetic fate mapping of Olig2 progenitors in the injured adult cerebral cortex reveals preferential differentiation into astrocytes. *J. Neurosci. Res.* **86**, 3494-3502.
Thioulouse, J. and Dray, S. (2007). Interactive multivariate data analysis in R with the ade4 and ade4TkGUI packages. *J. Stat. Soft.* **22**, 1-14.
Torii, M. and Levitt, P. (2005). Dissociation of corticothalamic and thalamocortical axon targeting by an EphA7-mediated mechanism. *Neuron* **48**, 563-575.
Uemura, M., Nakao, S., Suzuki, S. T., Takeichi, M. and Hirano, S. (2007). OL-protocadherin is essential for growth of striatal axons and thalamocortical projections. *Nat. Neurosci.* **10**, 1151-1159.
Vanderhaeghen, P. and Polleux, F. (2004). Developmental mechanisms patterning thalamocortical projections: intrinsic, extrinsic and in between. *Trends Neurosci.* **27**, 384-391.
Vue, T. Y., Aaker, J., Taniguchi, A., Kazemzadeh, C., Skidmore, J. M., Martin, D. M., Martin, J. F., Treier, M. and Nakagawa, Y. (2009). Sonic hedgehog signaling controls thalamic progenitor identity and nuclei specification in mice. *J. Neurosci.* **29**, 4484-4497.
Watanabe, K., Tamamaki, N., Furuta, T., Ackerman, S. L., Ikenaka, K. and Ono, K. (2006). Dorsally derived netrin 1 provides an inhibitory cue and elaborates the 'waiting period' for primary sensory axons in the developing spinal cord. *Development* **133**, 1379-1387.
Wilkinson, D. G. (1998). *In situ Hybridization, A Practical Approach*. Oxford, UK: Oxford University Press.
Xu, N.-J. and Henkemeyer, M. (2012). Ephrin reverse signaling in axon guidance and synapstogenesis. *Semin. Cell Dev. Biol.* **23**, 58-64.
Zhou, Q. and Anderson, D. J. (2002). The bHLH transcription factors OLIG2 and OLIG1 couple neuronal and glial subtype specification. *Cell* **109**, 61-73.

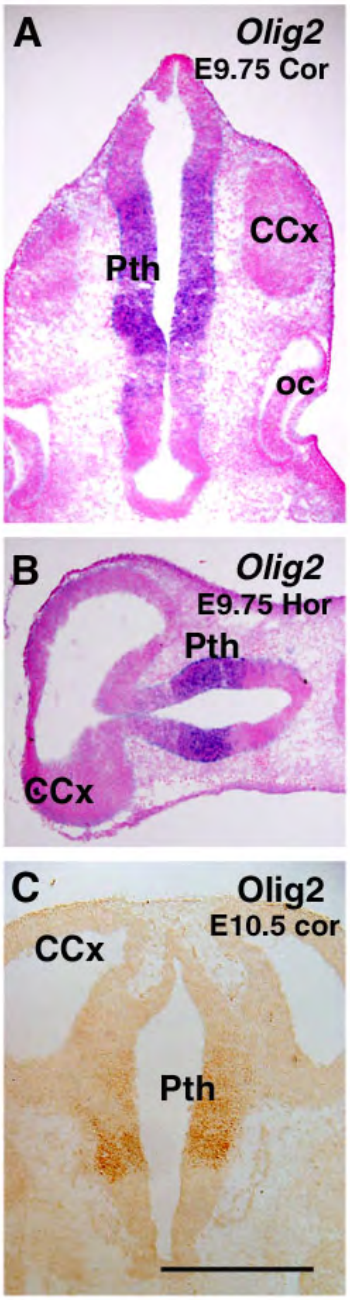

Supplementary Fig. 1 Expression of Olig2 in early diencephalon development
Expression of Olig2 was examined in the E9.75 (A,B) and E10.5 (C) diencephalon with *Olig2* ISH (dark blue) and Olig2 IHC (brown), respectively. A and C are coronal sections and B is a horizontal section. Note that Olig2 mRNA or protein is expressed in the diencephalon of these stages. Red in A and B is nuclear fast red for counter-staining. CCx, cerebral cortex. oc, optic cup. Pth, prethalamus. Bar in C = 500μm.

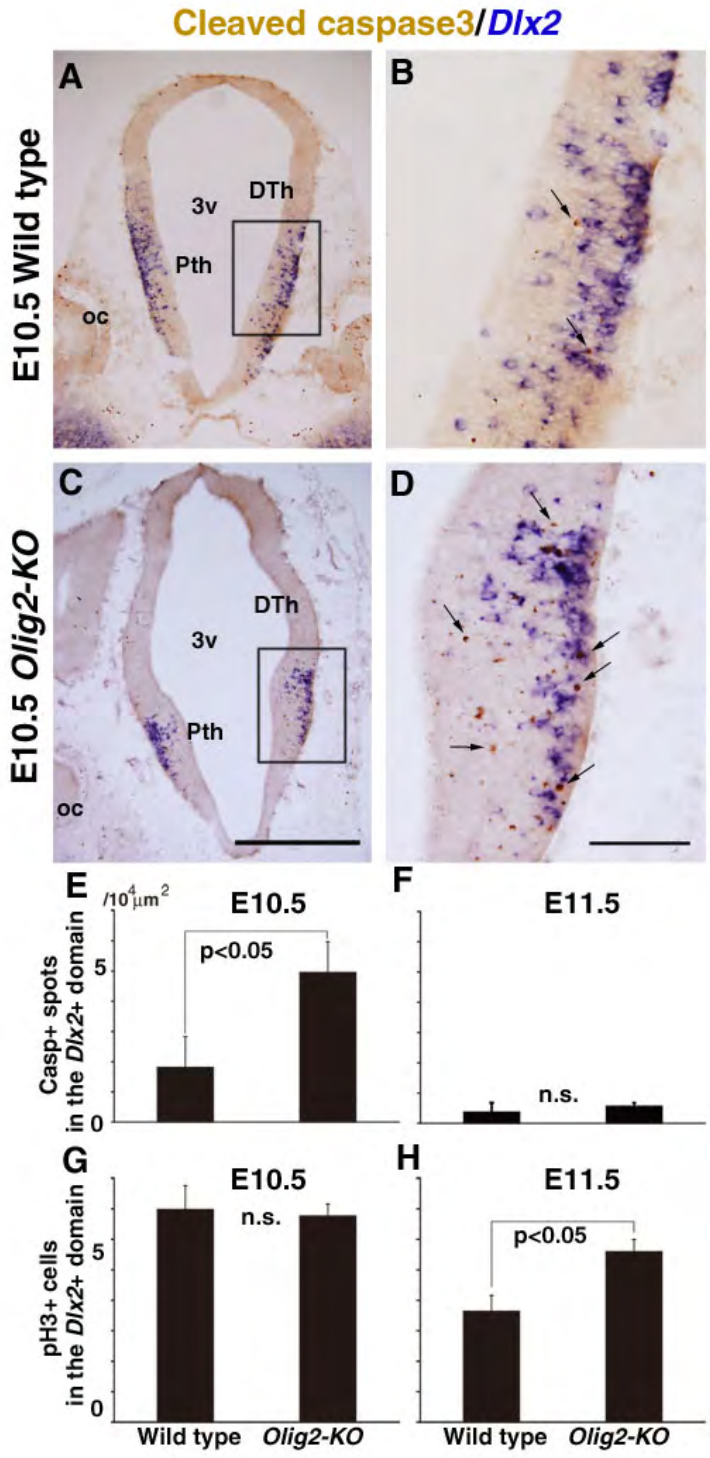

Supplementary Fig. 2 Apoptosis and proliferation in the prethalamus of *Olig2-KO* mice
A-D: E10.5 diencephalon of normal control (A,B) and *Olig2-KO* (C,D) was double-stained with *Dlx2* ISH and cleaved (activated) caspase-3 IHC. Caspase-3+ spots (arrows) were observed in the diencephalon, including the Dlx2+ prethalamus, and were more abundant in the *Olig2-KO* than in the control prethalamus. 3v, third ventricle. oc, optic cup. Bar in B = 200μm; in D = 100μm. E, F: Density of cleaved caspase-3+ spots in the E10.5 and E11.5 prethalamus. G,H: Density of pH3+ mitotic cells in the E10.5 and E11.5 prethalamus.

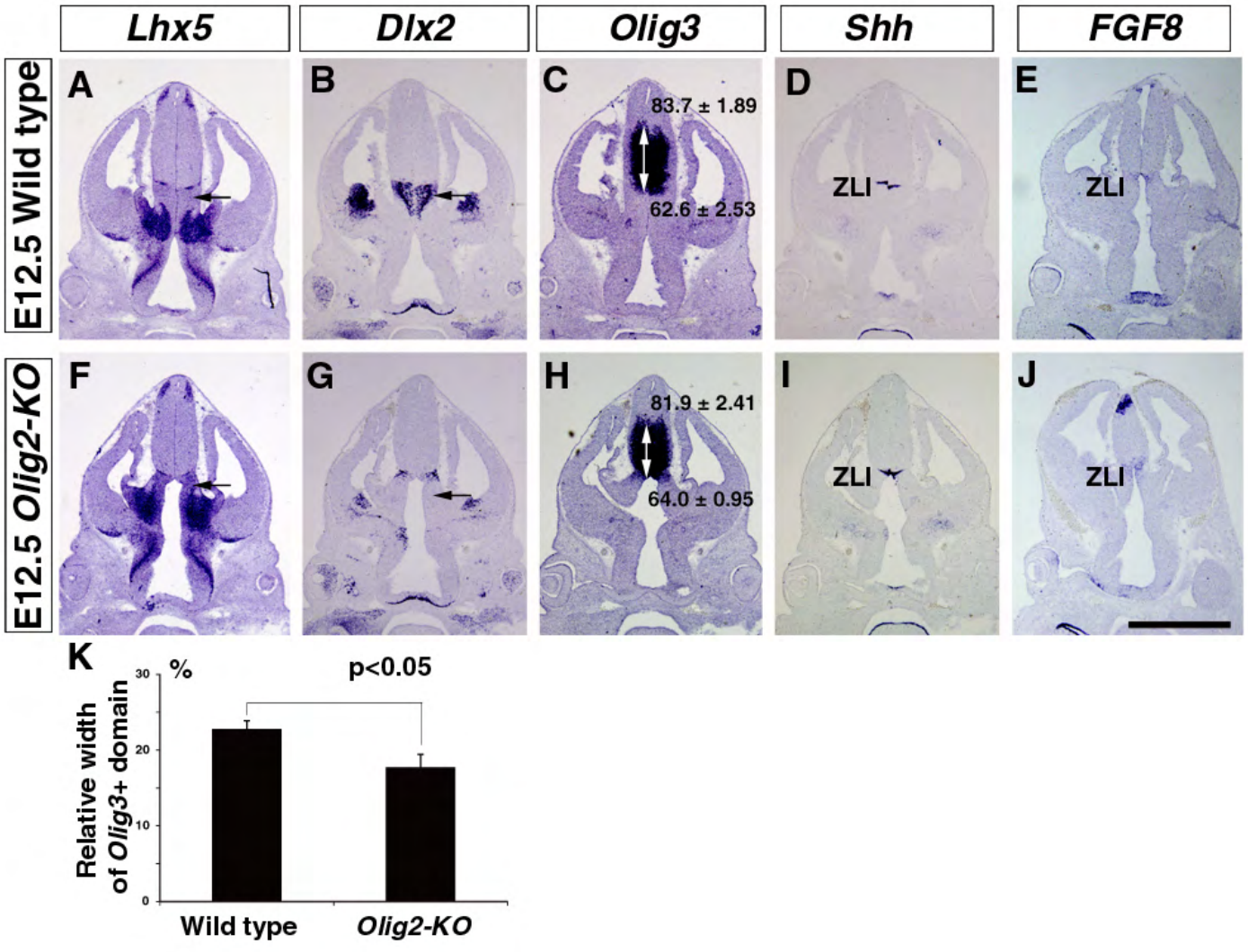

Supplementary Fig. 3 Expression of transcription factors and morphogen molecules in the E12.5 diencephalon
A-E: E12.5 wild-type. F-J: E12.5 *Olig2-KO*. Arrows in A, B, F, G indicate the prethalamus which shows hypoplasia. A, F: *Lhx5* is expressed in the dorsal border of the prethalamus and thalamic eminence while the main part of the prethalamus is devoid of *Lhx5* expression. In the *Olig2-KO* diencephalon, *Lhx5*-negative region is much smaller (F) than the control (A). B, G: *Dlx2* expression in the prethalamus. C, H: *Olig3* is mainly expressed in the dorsal thalamus. Double-direction arrows in images indicate an extend of Olig3+ domain, and numbers indicate the relative position of the dorsal and ventral borders, which are unchanged in *Olig2-KO* mouse (see text), while the relative width of the *Olig3*-expressing domain is slightly reduced in the *Olig2-KO* mouse (K). D, I: *Shh* expression is observed in the zona limitans intrathalamica (ZLI) in both wild-type and *Olig2-KO* mice. E, J: *FGF8* expression is mostly restricted to the rostralmost part of the diencephalon and ZLI shows very weak expression of *FGF8*, which is similar between wild-type and *Olig2-KO*. Bar = 1mm.

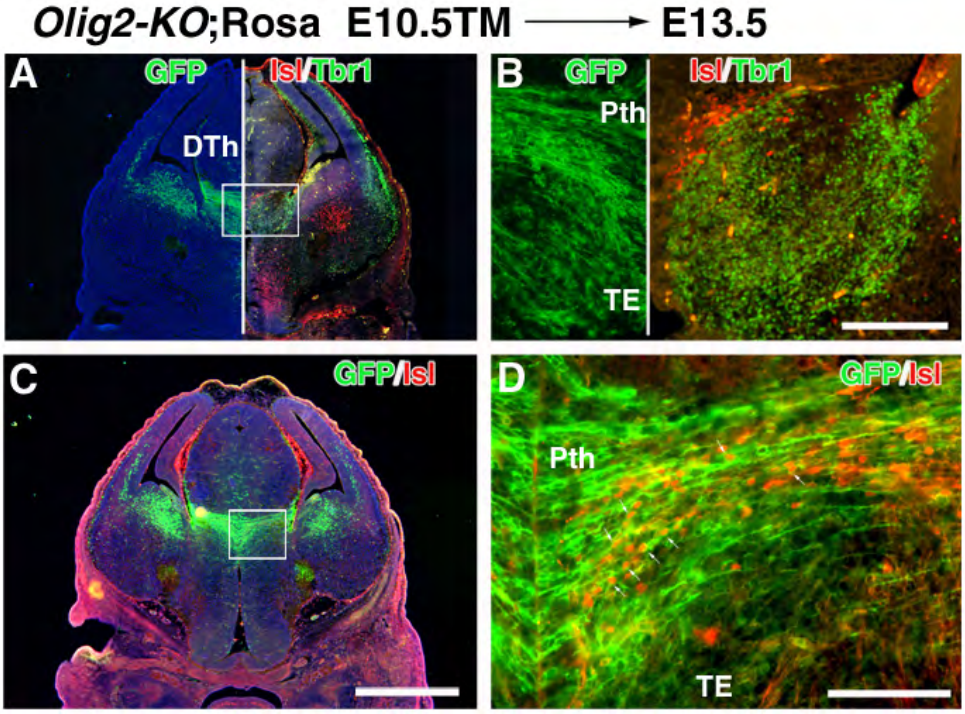

Supplementary Fig. 4 Dual phenotype of Olig2 lineage cells in the Olig2-KO diencephalon
E13.5 *Olig2-KO*;Rosa26^{GFP} mouse diencephalon with tamoxifen treatment at E10.5. Boxed areas in A and C are magnified in B and D, respectively. A, B: Composite pictures in which left and right halves are adjacent sections immunostained with GFP (green in left half), Islet1/2 (red in right half), and Tbr1 (green in right half) IHC. Note that GFP+ area shows Tbr1 and Islet1/2 expression. C, D: A section double-stained with anti-GFP and anti-Islet1/2 antibodies. Arrows in D indicate double-labeled cells. The results, together with those in Fig. 3, elucidate that Olig2 lineage cells in the *Olig2-KO* diencephalon are dual phenotypes, both prethalamus and thalamic eminence. Bars in C = 1mm; in D = 200μm.

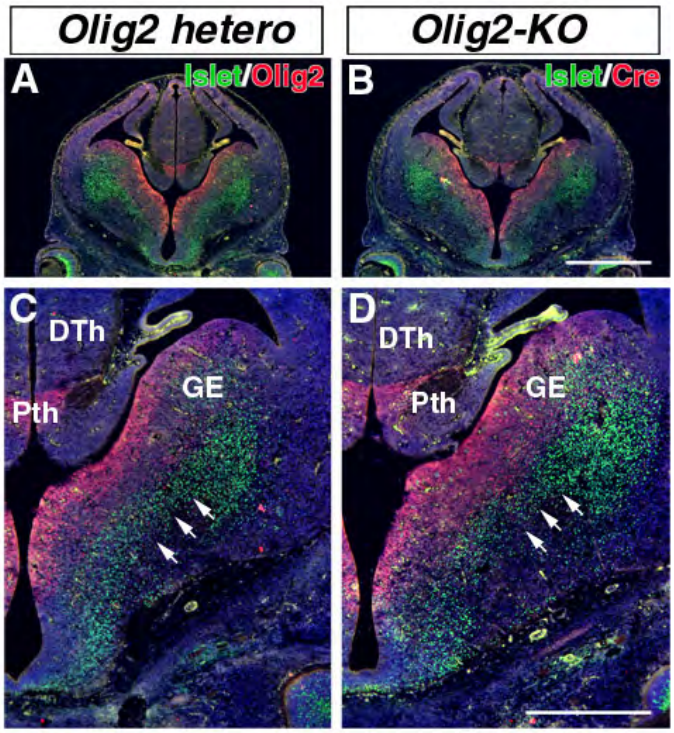

Supplementary Fig. 5 Normal arrangement of Islet1/2+ cells including corridor cells in the *Olig2-KO* ventral telencephalon
E13.5 forebrain is double-stained with Islet1/2 (green) and Olig2 (red in A and C) or CreER (red in B and D). Islet1/2+ cells are aligned dorsolaterally (arrows in C and D) in the ventral telencephalon, which contains corridor cells, in both Olig2 heterozygous and KO mice. Bars in B = 1 mm; in D =500μm.

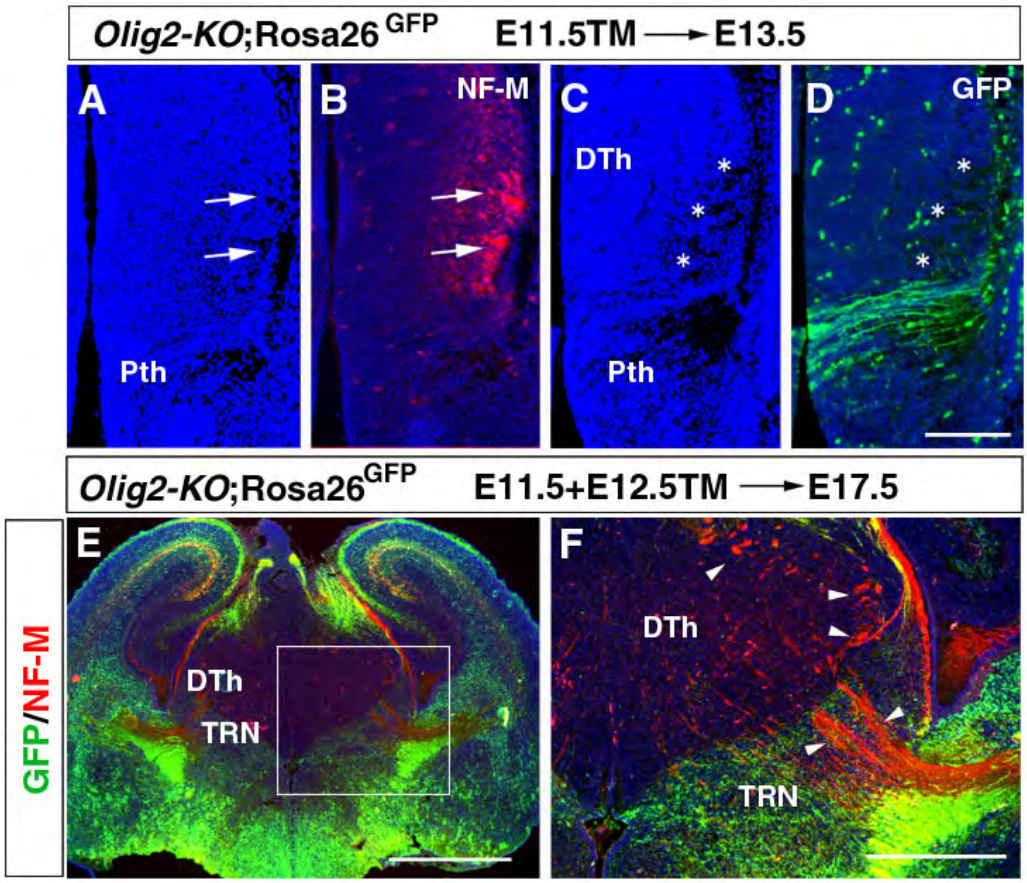

Supplementary Fig. 6 Distribution of Olig2 lineage cells and axons in the prethalamus
A-D: E13.5 dorsal thalamus of the *Olig2-KO*;Rosa26^{GFP} mouse with E11.5 TM treatment is stained by NF-M (B) or GFP (D) immunohistochemistry. Nuclear staining with Hoechst reveals small cell-free zones (arrows in A) that are filled with NF-M+ axons (B). However, when the adjacent sections are stained with anti-GFP antibody, which labels Olig2 lineage cells and processes, GFP+ processes are observed in the prethalamus (Pth) and the marginal zone of the dorsal thalamus (DTh in C), but not in cell-free zones in the dorsal thalamus. E, F: E17.5 diencephalon of the *Olig2-KO*;Rosa26^{GFP} with tamoxifen treatment at E11.5 and E12.5. Most of the NF+ axons (red) in the dorsal thalamus are not labeled with GFP, so that disorganized axons are not extended from Olig2 lineage neurons. Bar in D = 200μm; in E = 1mm; in F = 500μm.

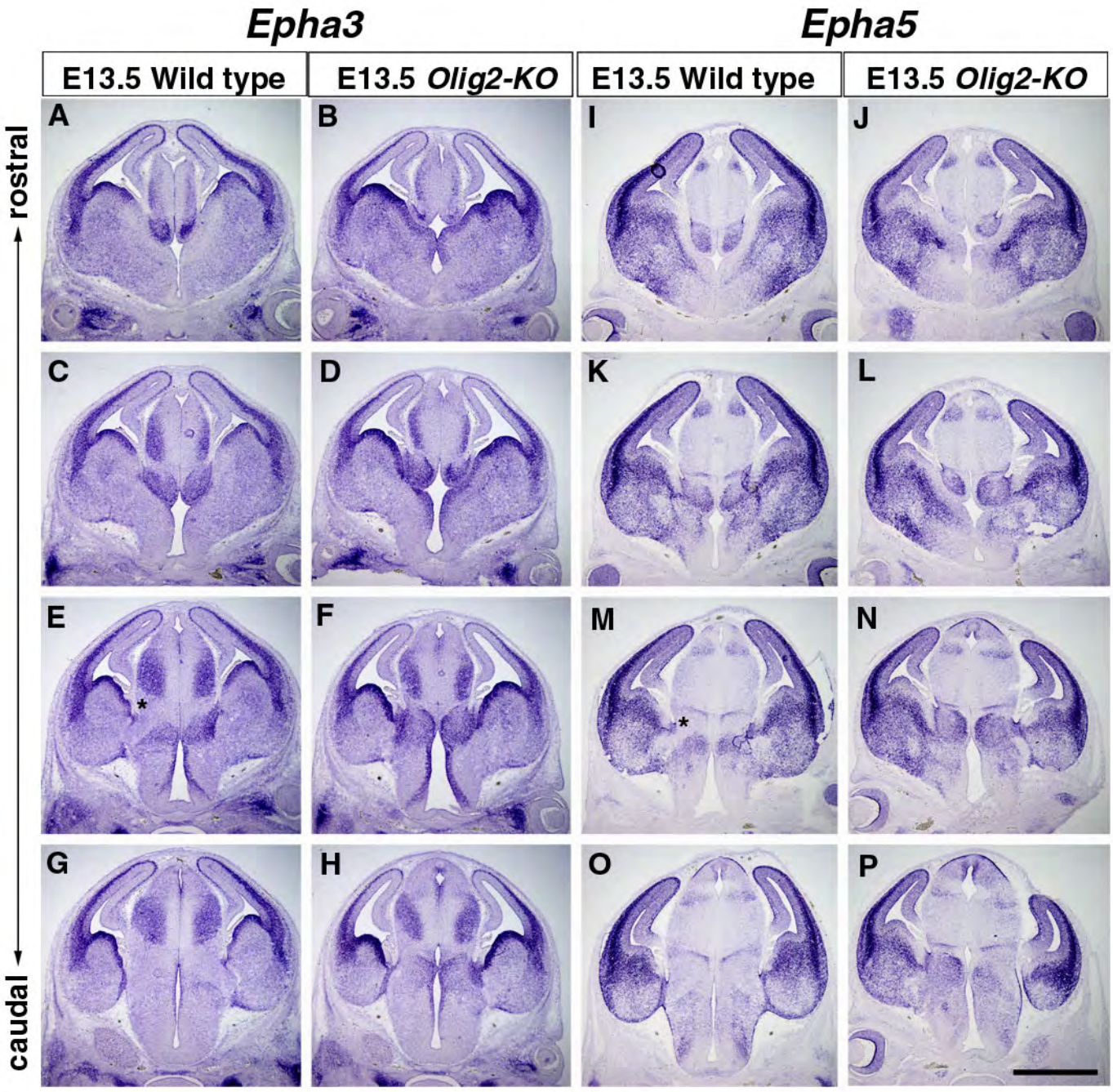

Supplementary Fig. 7 Details of *Epha3* and *Epha5* expression in the E13.5 diencephalon
Rostral to caudal arrangement of E13.5 forebrain stained with *Epha3* ISH (A-H) or with *Epha5* ISH (I-P) in the wild-type and *Olig2-KO* mice. Note that prethalamus in the wild-type is devoid of *Epha3* and *Epha5* expression that continues to the ventral telencephalon (asterisks in E and M). Such a *Epha*-negative region is missing in the *Olig2-KO* mouse. E, F, M and N are the same picture to Fig. 7A-D. Bar = 1mm.

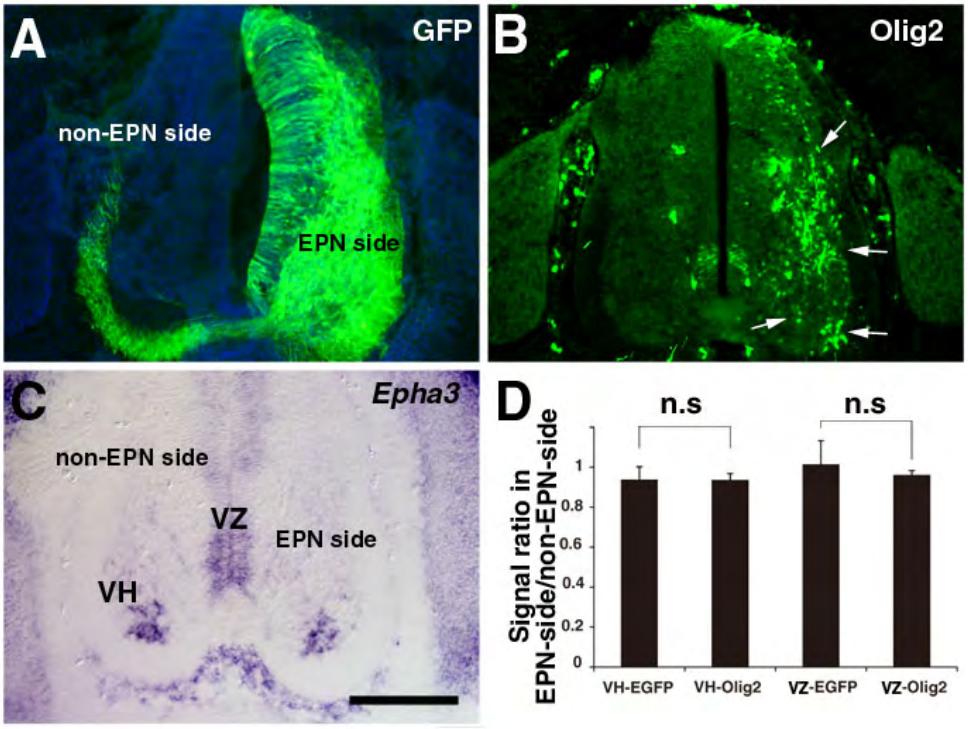

Supplementary Fig. 8 No effect of ectopic Olig2 on *Epha3* expression
Olig2 expression vector was electroporated to the E3 chick neural tube together with EGFP expression vector, and the spinal cord was analyzed at E6 to identify whether *Epha3* expression was affected by ectopic overexpression of Olig2. A, B: Serial sections of the E6 spinal cord with co-electroporation of GFP and Olig2. Ectopic Olig2 was indicated by arrows, which includes ventral horn (VH). C: *EphA3* expression was observed in the ventral VZ and VH. D: Ratio of signal intensity between electroporated (EPN) side (Olig2 and GFP or GFP alone) and non-electroporated (non-EPN) side was nearly 1, which means that *Epha3* expression was unaffected by ectopic Olig2. Bar in C = 200μm.